Activation of NF-κB by a novel, CDK4-regulated, nucleolar stress response pathway

Jingyu Chen[1]; Ian T Lobb[1]; Pierre Morin[1]; Sonia M Novo[1]; James Simpson[1]; Kathrin Kennerknecht[1], Fiona Oakley[2] and Lesley A. Stark[1]*

1. University of Edinburgh Cancer Research Centre, Institute of Genetics and Molecular Medicine, Western General Hospital, Crewe Rd., Edinburgh, Scotland EH4 2XU.

2. Liver Research Group, Institute of Cellular Medicine, 4th Floor, William Leech Building, Framlington Place, Newcastle University, Newcastle Upon Tyne, NE2 4HH

Corresponding Author:

*Lesley Stark

Edinburgh Cancer Research Centre,

Institute of Genetics and Molecular Medicine

Western General Hospital,

Crewe Rd.,

Edinburgh,

Scotland

Tel: 44 (0)131 651 8531

Email: Lesley.Stark@IGMM.ed.ac.uk

Running title: Nucleolar stress stimulates NF-κB signalling

Keywords: Nucleoli, RRN3, aspirin, NF-kappaB, NSAIDs, stress, P14ARF, CDK4, UBF.

Abstract

The nucleolus is a multifunctional organelle that plays a critical role in maintaining cellular homeostasis under stress. However, how nucleoli sense stress and coordinate specific phenotypic outcomes, remains poorly understood. Here, we identify a novel nucleolar stress response pathway that culminates in activation of NF-κB. Using multiple approaches, we show that specific disruption of the PolI complex stimulates NF-κB signalling. Unlike the paradigm of nucleolar stress, this stimulation is not caused by inhibition of rRNA transcription. We identify a novel mechanism by which specific stresses disrupt nucleoli involving CDK4 inhibition and consequently, UBF-p14ARF-dependent degradation of the PolI complex component, TIF-IA. We show this atypical nucleolar stress response is associated with a distinctive nucleolar architecture. Furthermore, we show it lies upstream of NF-κB signalling. Finally, we explore the relevance of this pathway in response to aspirin in human clinical samples and demonstrate a correlation between TIF-IA degradation and NF-κB pathway activation. Together, these data provide a conceptual advance in understanding of nucleolar stress response with therapeutic implications.

Introduction

The nucleolus is a highly dynamic sub-nuclear organelle that, in addition to its primary function as the hub of ribosome biogenesis, acts as a critical stress sensor and coordinator of stress response [1, 2]. The first step in ribosome biogenesis is transcription of pre-ribosomal RNA (pre-rRNA) by the RNA polymerase I (PolI) complex. Pre-RNA is then cleaved and assembled with ribosomal and accessory proteins to generate the 40S and 60S ribosomal subunits. This process is the most energy consuming in a cell and as such, is closely linked to metabolic and proliferative activity. If cells are exposed to stresses/insults that threaten this activity (e.g UV-C radiation, nutrient depletion, infection, DNA damaging or toxic agents), rRNA transcription is inhibited and a cascade of nucleolar events is triggered that will either allow the cell to repair and regain homeostasis, or, if the damage is too great, undergo cell death. The nucleolar proteome contains over 4500 proteins, more than half of which are involved in processes out-with ribosome biogenesis such as transcription, cell cycle regulation, chromatin structure, ubiquitin modification, apoptosis and proliferation[3]. It is thought to be the differential release of these regulatory proteins to the nucleoplasm/cytoplasm in response to stress that ultimately determines cell fate. Outcomes that have been linked with nucleolar perturbation include differentiation, cell cycle arrest, autophagy, DNA repair, senescence and apoptosis[4].

Although it is well established that nucleoli play an important role in the maintenance of cell homeostasis, the mechanisms that coordinate stress effects on the PolI complex, and integrate these effects into individual phenotypic outcomes, remain poorly understood. The most recognised downstream consequence of nucleolar stress is stabilisation of p53 and the pathway leading to this stabilisation has been widely reported [5-7]. However, it is increasingly apparent that perturbation of nucleolar function can regulate cell phenotype in a p53 independent manner[8]. Spatial proteomic studies, demonstrating hundreds of nucleolar

proteins with p53 independent functions relocate from the nucleolus in response to stress, also support this notion[9, 10].

Similar to p53, the NF-κB transcription factor plays a critical role in maintaining cellular homeostasis under stress[11]. The most abundant form of NF-κB is a heterodimer of the p50 and RelA polypeptides, which is generally bound in the cytoplasm by the inhibitor, IκBα [12]. Upon exposure of the cell to a myriad of stress signals, IκBα is degraded allowing NF-κB to translocate to the nucleus where it regulates expression of target genes[13-15]. The most recognised NF-κB stimuli are pro-inflammatory cytokines, which induce rapid/transient NF-κB activation by mechanisms that are well-defined. In contrast, stress stimuli (including serum deprivation, UV-C radiation and chemotherapeutic/preventative agents) induce slow, prolonged activation of NF-κB by mechanisms that remain poorly understood.

A common denominator of stresses that activate NF-κB is disruption of nucleoli (some of which are summarised in Supplemental Table 1)[16-18]. Furthermore, proteins that have a role in stress-mediated activation of NF-κB reside within this organelle. For example, CK2, which forms part of the PolI complex and facilitates rDNA gene transcription, phosphorylates IκB in response to UV-C[19, 20]. EIF2α is also a nucleolar protein that plays a role in NF-κB activation in response to multiple stresses[21, 22]. Previous work in this lab has shown that post induction, RelA can accumulate in nucleoli[23, 24]. However, the relationship between stress-mediated nucleolar disruption and activation of the cytoplasmic NF-κB pathway has not yet been considered.

Here we define a novel, p53 independent nucleolar stress response pathway that triggers activation of NF-κB. We firstly show that artificial disruption of the PolI complex induces degradation of IκB and consequently, increased transcription of NF-κB target genes. Unlike classical nucleolar stress, this effect is not caused by inhibition of rRNA transcription. We show that multiple stress stimuli of NF-κB induce degradation of the critical PolI com-

plex component, TIF-IA. We identify an upstream mechanism for this degradation involving CDK4-UBF-p14ARF, and show that increased nucleolar area and activation of the NF-κB pathway lie downstream of this degradation. Finally, we show an association between TIF-IA degradation and stimulation of NF-κB in response to pharmacological concentrations of aspirin in fresh, surgically resected human colorectal tumours, suggesting this pathway is triggered in a whole tissue setting and has relevance to the anti-tumour effects of the agent.

Results

Direct disruption of nucleolar function activates the NF-κB pathway

To explore the link between stress effects on nucleoli and activation of NF-κB signalling we started by directly inhibiting upstream binding factor (UBF), an essential component of the PolI pre-initiation complex. Such inhibition was previously used by Rubbi and Milner to show nucleolar stress stabilises p53[5]. To disrupt UBF activity we initially utilised an inactive mutant (Flag-UBF-S388G) that is known to block rRNA transcription[25]. We found that compared to expression of wild type UBF, expression of the mutant induced a significant increase in nuclear RelA, increased S536 phosphorylated RelA (an independent marker for cytoplasmic activation of the NF-κB pathway) and a greater than 5 fold increase in NF-κB-driven transcription (Figs. 1a to c). siRNA to UBF confirmed that inactivation of this protein stimulates the NF-κB pathway, as evidenced by increased nuclear RelA, S536 phosphorylated RelA and an increase in NF-κB-driven transcription comparable to that observed when cells were treated with the classic NF-κB stimulus, TNF (Fig. 1d and Supplemental Fig. 1a). To determine whether this effect was a general consequence of PolI disruption, or restricted to inhibition of UBF, we utilised siRNA to two further complex components, PolR1A (RPA194 subunit) and TIF-IA (Rrn3p). We found depletion of these proteins also induced degradation of IκB, increased $pRelA^{S536}$ and increased NF-κB-driven transcription (Figs. 1d and e and Supplemental Fig. 1a).

To further confirm that directly disrupting nucleoli activates NF-κB signalling we utilised a reporter plasmid in which transcription of the luciferase gene is driven by the full length promoter of the classic NF-κB target, IκBα. Figure 1f demonstrates that depletion of UBF induces a more than five-fold increase in transcription from the IκBα promotor. Depletion of TIF-IA also caused a significant increase in IκBα transcription. However, the increase in trabscription was abrogated when an equivalent reporter plasmid lacking κB sites

was utilised. qRTPCR confirmed a significant increase in transcription of IκBα and another NF-κB target gene, Bcl-xl in response to PolI complex disruption (Fig. 1g).

As would be expected, siRNA to UBF, PolRIA and TIF-IA inhibited rRNA transcription (Supplemental Fig. 1b). To explore the role of this inhibition in activation of the NF-κB pathway we utilised low dose actinomycin D (specifically inhibiting PolI activity) and two highly specific small molecule inhibitors of this process, CX5461 and BHM-21[26, 27]. We found all these agents induced a significant decrease in rRNA transcription (Supplemental Fig. 1c). They are also known to stabilise p53[26, 27]. However, they had no effect on NF-κB-driven transcription (Fig. 1h).

Given that disrupting nucleolar function causes dramatic changes to the nuclear proteome[10], we considered that depleting PolI complex components may stimulate NF-κB transcriptional activity in the absence of cytoplasmic release of NF-κB. However, blocking cytoplasmic to nuclear translocation of NF-κB, using cells we generated that constitutively express super repressor (non-degradable) IκBα, blocked the effects of TIF-IA/UBF depletion on NF-κB-driven transcription (Fig. 1i and supplementary Fig. 1d). These data confirm that IκBα degradation is an essential step in nucleolar stress mediated induction of NF-κB transcriptional activity.

Taken together, these data indicate that direct disruption of the PolI complex activates the cytoplasmic NF-κB pathway. They also suggest that unlike the paradigm of nucleolar stress, this activation is not a consequence of inhibition of rRNA transcription per se, but due to a specific type of PolI complex disruption. To test this hypothesis, and further explore the link between nucleoli and stress-mediated activation of NF-κB, we investigated the effects of NF-κB stress stimuli on proteins of this complex.

TIF-IA degradation and increased nucleolar size in response to stress-stimuli of the NF-κB pathway

TIF-IA is known as the PolI complex component that senses stress/environmental signals and transfers these signals to the PolI transcription machinery[28, 29]. It also plays an important role in nucleolar structure and in the regulation of cell growth and death. Therefore, we started by investigating this protein. The first stress stimuli we utilised was aspirin as we are interested in its pro-apoptotic activity and have shown it stimulates NF-κB in the delayed/prolonged manner characteristic of multiple inducers[30].

Surprisingly, we found aspirin not only induced a decrease in phosphorylated TIF-IA (at the critical Ser649 residue), which is a known response to environmental changes, but also a substantial reduction in native TIF-IA (Fig.2a), which is *not* a reported stress response. This reduction was observed in multiple cell types and was independent of p53 status (supplemental Figs 2a and b). It was also extremely rapid, preceding degradation of IκB and nuclear translocation of RelA (Figs. 2a and b). qRT-PCR and cyclohexamide run on assays revealed that the reduction was not a consequence of reduced gene transcription, but caused by increased turnover of the protein (Fig. 2c and supplemental Figs. 2c and d). UV-C also induced TIF-IA degradation prior to degradation of IκB (Fig. 2d and supplemental Fig. 2e). In contrast, CX-5461, BMH21, actinomycinD and TNF had a minimal effect on TIF-IA levels (Fig. 2e).

The hallmarks of classical nucleolar stress are inhibition of rRNA transcription and segregation of nucleolar proteins[1]. As aspirin and actinomycinD had differing effects on TIF-IA, we considered they may have differing effects on these hallmarks. qRTPCR for the 47S pre rRNA transcript, 5-fluorouridine (FUrd) run on assays and immunocytochemistry revealed that while both agents caused a significant reduction in rRNA transcription and re-localisation of nucleolar marker proteins, they had distinct effects on nucleolar architecture

(Figs. 2f to j and supplemental Fig. 2f). Aspirin induced a decrease in nucleolar number and a significant *increase* in nucleolar area. In contrast, actinomycinD induced a significant *reduction* in nucleolar area (Fig. 2h). Time course studies indicated that aspirin effects on rRNA transcription and nucleolar area paralleled loss of TIF-IA, suggesting this distinctive nucleolar phenotype may be associated with this loss (Fig. 2i). UV-C induced a similar nucleolar phenotype to aspirin, in keeping with this suggestion (Fig. 2j).

Aspirin and UV-C generate ceramide, a crucial lipid second messenger that induces its cytotoxic effects through activation of NF-κB[31-34]. On examination we found that the C2 and C6 soluble forms of ceramide also induced degradation of TIF-IA (Fig. 2k and supplemental Fig. 2e). Furthermore, this occurred in parallel with enlargement/segregation of nucleoli and degradation of IκB (Fig. 2k).

Taken together, these data indicate that specific stimuli of the NF-κB pathway induce a distinctive type of nucleolar stress that is associated with degradation of TIF-IA and enlargement/segregation of nucleoli. They also suggest a possible link between this distinctive nucleolar phenotype and stimulation of the NF-κB pathway. To help clarify this link, we investigated the mechanism underlying stress-mediated TIF-IA degradation.

Identification of p14ARF as a regulator of TIF-IA stability.

Previous studies demonstrated that basal TIF-IA is regulated by proteasomal degradation, facilitated by MDM2 or Sug-1[16, 35]. However, we found that chemical inhibition of the proteasome (using MG132 or lactacystin) could not block aspirin-mediated degradation of TIF-IA (Fig. 3a and supplemental Figs 3a to c). We also found that, although the MDM2 inhibitor Nutlin-3 increased basal TIF-IA as reported[16], it had no effect on aspirin-mediated degradation of the protein (Supplemental Fig. 3c). Similarly, the basal interaction observed between TIF-IA and Sug-1 did not change substantially after aspirin exposure (Supplemental Fig. 3d).

These data eliminated proteasomal degradation and so we considered a role for lysosomal degradation. However, we found that chemically inhibiting lysosome activity alone also had no effect on aspirin-mediated TIF-IA degradation (Fig. 3a and Supplementary Figs e and f). Indeed, we found that the observed degradation of TIF-IA could only be blocked by inhibiting proteasomal and lysosomal activity together, indicating redundancy in the degradation pathway (Fig. 3a).

As lysosomal degradation is not reported within nucleoli, we generated a series of GFP-tagged deletion and site mutants to investigate the cellular localisation of TIF-IA degradation, and to further explore the mechanism underlying this degradation (Supplementary Fig. 3g). These data revealed that amino acids 94-204 are sufficient for aspirin-mediated degradation of TIF-IA, but that the recognised phosphorylation sites within this region (S170/2, S199 and T200) are dispensable (Fig. 3b and supplemental Fig. 3g). They also revealed that GFP-TIF-IA 94-302 and 94-204, which localise in the nucleoplasm/cytoplasm, undergo aspirin-mediated degradation comparable to that of full length protein (Fig. 3b and supplementary Fig. 3g for GFP control).

In a related study in the lab, aimed at identifying aspirin effects on the nucleolar proteome, we noted that an early response to this agent was a decrease in nucleolar p14ARF (unpublished data). This was of particular interest as the p14ARF tumour suppressor is known to play a role in cytoplasmic shuttling of PolI complex components[36]. It also regulates rDNA transcription in a p53/MDM2 independent manner and influences NF-κB signalling[37, 38]. Therefore, we investigated the role of this protein and found that overexpression of p14ARF enhanced aspirin-mediated degradation of TIF-IA while siRNA depletion abrogated this effect, especially at lower doses of the agent (Figs. 3c and d). Immunocytochemical analysis confirmed that the significant reduction in TIF-IA observed in response to aspirin in cells transfected with control siRNA, was lost in cells transfected with siRNA to p14ARF

(Fig. 3e). Importantly, TIF-IA accumulated within nucleoli in p14ARF depleted cells, suggesting a role for p14ARF in nucleolar shuttling of the protein (Fig. 3e). In keeping with this suggestion, immunoprecipitation assays revealed that TIF-IA and p14ARF interact and that this interaction is enhanced in response to aspirin in a dose and time dependent manner (Fig. 3f and supplementary Fig. 3h)

CDK4 inhibition lies upstream of stress-mediated TIF-IA degradation

A common early response to stress stimuli of NF-κB is reduced activity of the cyclinD1-CDK4/6 complex (Supplementary Figs. 2e and 3a and b)[39]. This is of interest as CDK4/6 targets UBF, which complexes with both TIF-IA and p14ARF[37, 40]. Therefore, we considered that CDK4 inhibition may lie upstream of stress effects on p14ARF-TIF-IA[40, 41] and that UBF acts as a bridging protein in the process. To test this suggestion, we initially examined the link between CDK4 and TIF-IA using a highly specific CDK4 inhibitor (CDK4i). We have previously shown this inhibitor mimics stress effects on the NF-κB pathway [39]

In keeping with our hypothesis, immunoblot analysis indicated that CDK4i (and an independent CDK4 inhibitor, PD0332991) induced degradation of TIF-IA (Figs. 4a and b and Supplemental Fig. 4a). Interestingly, immunocytochemistry clearly demonstrated that TIF-IA localises to the cytoplasm in response to lower dose CDK4i (Fig. 4c). It also indicated that inhibition of CDK4 activity induces the same distinct nucleolar phenotype as stress stimuli of the NF-κB pathway i.e reduced nucleolar number, increased nucleolar size, segregation of nucleolar marker proteins and inhibition of rRNA transcription (Fig. 4d and Supplemental Figs 4b and c).

When we examined the mechanism underlying CDK4i-mediated TIF-IA degradation we found that it paralleled the mechanism underlying stress-mediated degradation of the protein i.e, it was dependent on both proteasomal and lysosomal pathways and was evident in mutants that locate out-with nucleoli (GFP-TIF-IA 94-204, 94-302). (Supplemental Figs. 4d

to f). Importantly, both immunoblot and immunocytochemical analysis demonstrated that it was also absolutely dependent on p14ARF (Figs. 4e and f). Indeed (as with stress stimuli), in the absence of p14ARF, TIF-IA accumulated in nucleoli (Fig. 4f).

Having established that inhibition of CDK4 mediates degradation of TIF-IA in a p14ARF dependent manner, we next investigated the role of UBF. We found that both CDK4i- and aspirin-mediated degradation of TIF-IA were paralleled by dephosphorylation of UBF at the known CDK4 phosphorylation site, S484 (Fig. 4g). We also found that siRNA silencing of UBF substantially abrogated aspirin- and CDK4i-mediated TIF-IA degradation (Fig. 4h). In contrast, silencing of PolRIA had no effect, suggesting this abrogation was specific and not a general consequence of PolI complex disruption (Fig. 4h).

To further explore the role of UBF S484 de-phosphorylation, we examined the effects of aspirin and CDK4i on TIF-IA degradation in cells expressing UBF mutated at this site. SW480 cells were depleted for UBF then transfected with plasmids expressing either wild type UBF (Flag-UBFWT) or an S484 mutant that cannot be phosphorylated (Flag-UBF S484A). As would be expected from previous results (Fig. 4f), we found that depletion of UBF alone abrogated aspirin and CDK4i-mediated TIF-IA degradation (Fig. 4i and Supplemental Fig. 4g). We also found that this degradation was enhanced by expression of wild type UBF, but completely blocked by expression of the S484A mutant (Fig. 4i and Supplemental Fig. 4g). We did predict that, as it is constitutively dephosphorylated, expression of the mutant alone may mimic the effects of stress on TIF-IA. However, basal TIF-IA was similar in cells expressing wild type and mutant protein.

Taken together, these data suggest that stress mediated inhibition of CDK4 causes p14ARF dependent degradation of TIF-IA, and that aa484 of UBF is critical for this process.

TIF-IA degradation is directly linked to increased nucleolar area and stimulation of the NF-κB pathway

The results presented so far indicate that specific disruption of the PolI complex activates NF-κB signalling. They also reveal a novel mechanism by which the PolI complex is disrupted in response to stress and suggest this mechanism may lie upstream of NF-κB pathway activation. To further explore this relationship, we next blocked stress-mediated TIF-IA degradation using siRNA to p14ARF, then examined the downstream consequences. Figures 5a and b clearly indicate that the aspirin-induced increase in nucleolar area, degradation of IκB and nuclear/nucleolar accumulation of RelA, observed in cells transfected with control siRNA, are completely abrogated in cells transfected with siRNA to p14ARF. Inhibiting degradation of TIF-IA in this manner also blocked CDK4i-mediated nucleolar enlargement, degradation of IκB and nuclear accumulation of RelA (Figs. 5c and d). An independent siRNA confirmed that depletion of p14ARF blocks aspirin-mediated degradation of TIF-IA and IκBα (Supplemental Fig. 4h). In keeping with our previous studies showing stimulation of NF-κB pathway is necessary for aspirin-mediated apoptosis[30], we found that (unlike loss of p53[42]), P14ARF depletion also blocked the apoptotic effects of aspirin (Fig. 5e).

As p14ARF has previously been shown to regulate nuclear NF-κB activity, we did consider that siRNA to this protein could inhibit activation of the NF-κB pathway downstream of nucleolar disruption (Rocha et al., 2003). To test this possibility, we mimicked the effects of stress on the PolI complex (using siRNA to UBF) then analysed NF-κB activity in the presence and absence of p14ARF. We found that loss of PolI complex integrity activated NF-κB signalling to the same extent in the presence and absence of p14ARF (Supplemental Fig. 4i). These data indicate that in this stress response pathway, the role of p14ARF is upstream of PolI complex disruption.

To definitively establish a connection between inhibition of CDK4 activity, disruption of the PolI complex and activation of the NF-κB pathway we next utilised the UBF-S484A mutant that blocks aspirin and CDK4i-mediated TIF-IA degradation (Fig. 4i). SW480 cells were transfected with control or UBF siRNA prior to overexpression of Flag-UBF-WT or -S484A. Quantitative immunocytochemistry revealed that for both control and UBF siRNA, CDK4i induced a significant increase in nuclear levels of RelA in cells transfected with wild type UBF, but not in those transfected with the S484A phospho-mutant (Fig. 5h and supplemental Fig. 4j). It also confirmed that depletion of UBF mimics the effects of stress and induces a significant increase in nuclear RelA alone. Taken together, these data provide extremely compelling evidence that stress disrupts the PolI complex through CDK4-UBFS484-P14ARF-TIF-IA and that this disruption activates the NF-κB pathway.

Based on the data presented here and that of others, we propose the model outlined in Figure 5i. We suggest that stress-mediated inhibition of CDK4 causes P14ARF to export TIF-IA for degradation, and that UBF acts as an intermediatory in this process. We propose that the resultant changes in nucleoli cause the release of specific proteins into the cytoplasm, which induce degradation of IκBα, p536 phosphorylation/nuclear translocation of RelA and consequently, changes in the NF-κB-driven gene transcription programme.

Relationship between TIF-IA degradation and stimulation of NF-κB signalling in human clinical samples

Overwhelming evidence indicates that aspirin has anti-tumour activity and the potential to prevent colorectal and other cancers[43-45]. To investigate the clinical significance of our results with regards to this activity, and to determine whether this novel nucleolar stress response pathway has relevance in a whole tissue setting, we treated biopsies of fresh, surgically resected human colorectal tumours with pharmacological doses (0-100 μM, 1h) of aspirin *ex vivo* (Fig. 6a). This aspirin concentration is comparable to salicylate levels we

measured in plasma from patients given a short course of analgesic doses of aspirin [30]. It is also well within the reported therapeutic range (0.1-3mM).

Western blot analysis indicated that low dose aspirin induces TIF-IA degradation (> 2 fold reduction in protein levels) in over 50% of human colorectal cancers (4/7) (Fig. 6b). Low dose aspirin also activated the NF-κB pathway (as indicated by a significant increase in the percentage of cells with $pRelA^{536}$ staining) in 50 % of tumours (Fig. 6c). Importantly, for individual tumours, there was a very strong inverse correlation (r^2=-0.85, n=6) between aspirin effects on TIF-IA protein levels and on phosphorylation of RelA (Fig. 6d). These data confirm that aspirin causes PolI complex disruption and activates the NF-κB pathway in primary human tumours and suggests a strong relationship between these two events in a whole tissue setting. These data have far reaching implications for understanding of the anti-tumour effects of this agent.

Discussion

The work presented here has great significance as we identify a novel nucleolar stress response pathway that activates NF-κB signalling. We show that unlike the paradigm of nucleolar stress, NF-κB activity is not triggered by inhibition of rRNA transcription per se, but by a distinct form of PolI complex disruption that is characterised by degradation of the critical PolI complex component, TIF-IA. We demonstrate the relevance of this pathway in vivo using human clinical samples and show it may contribute to the anti-tumour effects of aspirin. These data shed new light on the mechanisms by which nucleoli sense stress and coordinate the downstream consequences.

NF-κB plays a critical role in coordinating cellular response to a myriad of stresses. However, the question of how such a wide range of insults are sensed, then signal to the cytoplasmic NF-κB complex, has remained largely unanswered. Here we present compelling

evidence to suggest that disruption of nucleolar integrity activates NF-κB signalling. Firstly, we show that specifically disrupting the PolI complex causes degradation of IκBα, S536 phosphorylation and nuclear translocation of RelA, increased NF-κB-driven transcription and increased transcription of NF-κB target genes. We then show that multiple stress stimuli of NF-κB disrupt PolI complex integrity by inducing degradation of TIF-IA. Furthermore, we show that blocking the effects of these stimuli on the PolI complex abrogates their effects on the NF-κB pathway. Finally, we demonstrate a correlation between TIF-IA degradation and NF-κB pathway activation in biopsies of human colorectal tumours. Together, these data provide a potential mechanism by which multiple stresses can converge on the NF-κB pathway and thus, a novel means of regulating cellular homeostasis.

Specific disruption of the PolI complex causes cell cycle arrest[46], as do CDK4 inhibition and stress stimuli of NF-κB[47]. Therefore, we did consider that it is this cell cycle arrest that stimulates NF-κB signalling rather than nucleolar disruption *per se*. However, CX5461 and BMH21 induce cell cycle arrest[48] but we show they have no effect on NF-κB-driven transcription. Furthermore, we have previously shown that inhibiting the cell cycle does not mimic the effects of CDK4i on nucleoli or on the NF-κB pathway[49]. Therefore, we conclude that activation of the NF-kB pathway is a direct consequence of loss of nucleolar integrity.

In the classic nucleolar stress response pathway, inhibition of rRNA transcription triggers cytoplasmic release of RPL11/RPL5 which inhibits MDM2 to stabilise p53[27, 50]. We demonstrated that specifically inhibiting rRNA transcription has no effect on NF-κB-driven transcription. Therefore, we suggest that in this alternate pathway, it is loss of PolI complex integrity itself that triggers release of nucleolar proteins and ultimately, activation of NF-κB. The nature of the nucleolar proteins that stimulate the cytoplasmic NF-κB are currently unknown but CK2 is an excellent candidate as it is found as part of the PolI complex[19] and

phosphorylates IκBα in response to UV-C[20]. Another kinase of interest is NIK (NF-κB inducing kinase), which acts upstream of the IkappaB kinase (IKK) complex and is known to shuttle through nucleoli[51]. The role of these candidates will be the focus of future studies.

The mechanism reported for stress-mediated TIF-IA inactivation is modulation of its phosphorylation status, and a number of signalling cascades responsible for this modulation have been described [52]. The downstream consequences have also been well described. That is, nucleolar fragmentation and stabilisation of p53[52]. Here we report a novel pathway by which nucleoli sense and respond to stress which involves inhibition of CDK4 and ultimately, degradation of TIF-IA. We also provide compelling evidence to show that the downstream consequences of inactivating TIF-IA by this mechanism are nucleolar enlargement and activation of NF-κB. Together, these data indicate that the method by which TIF-IA is inactivated is important for governing the downstream molecular and phenotypic effects of nucleolar stress.

We show stress-mediated TIF-IA degradation is causally involved in increased nucleolar size, decreased nucleolar number, reduced rRNA transcription and apoptotic cell death. These findings are contradictory to the belief used widely by pathologists that increased nucleolar size in tumours is a marker for enhanced rRNA transcription and increased cell proliferation. In keeping with our findings, Fatyol et al found that MG132 induces a significant increase in nucleolar volume while inhibiting rRNA transcription and mediating cell death [35]. Similarly, Bailly et al found that the NEDD8 inhibitor, MLN4924, causes an increase in nucleolar size while inducing cell death, although in this case there was no effect on rRNA transcription [53]. These data bring into question the use of nucleolar size as an absolute marker of cell proliferation in diagnostic pathology.

In steady state conditions TIF-IA shuttles dynamically between the nucleolus, nucleoplasm and cytoplasm, but the mechanisms that govern this shuttling remain unclear[54].

Our finding that GFP-tagged TIF-IA mutants that locate out-with nucleoli are degraded in response to aspirin/CDK4i, and that depletion of p14ARF blocks this degradation and causes nucleolar accumulation of the protein, suggests that P14ARF acts by transporting TIF-IA to the cytoplasm to be degraded. These data are in keeping with previous studies showing p14ARF regulates the sub-cellular localisation of the PolI complex component TTF-I [55].

Uncontrolled rRNA transcription and nucleolar dysfunction are emerging as key factors in cancer aetiology and small molecules that inhibit this activity are currently the focus of intense scrutiny[27,56]. Both aspirin and CDK4 inhibitors are known to have potent anti-tumour activity and are in clinical trials. However, their precise mechanism of action remains unclear. Here we make the novel observation that these agents inhibit rRNA transcription, identifying a new mode of action. It will now be of interest to identify the signals that govern p14ARF export and degradation of TIF-IA, so that this pathway can be exploited for the design of safer, more effective chemopreventative and therapeutic agents.

In summary, the data presented here open up new avenues of research into nucleolar regulation of NF-κB signalling and regulation of TIF-IA stability under stress. They also shed further light on the complex mode of action of CDK4 inhibitors, aspirin and related non-steroidal anti-inflammatory drugs (NSAIDs).

Methods

Cell lines and treatments

Human SW480, HRT18, RKO and HCT116 colon cancer cells, PNT pancreatic cells and Hela Cervical cancer cells, are available from the American Type Culture Collection (ATCC). The p53 null derivative of HCT116 ($HCT116^{p53-/-}$) was a gift from Professor B Vogelstein (John Hopkins University School of Medicine, USA) and has previously been described[58]. HRT18SR, a derivative of HRT18 cells that constitutively express a non-degradable IκBα were generated in this lab and have been described[30]. All cells lines were maintained at 5%

CO2 in growth medium (Gibco) supplemented with 10% fetal calf serum (FCS) and 1% penicillin/streptomycin. Medium used was: SW480: Leibovitz's L-15: PNT, RKO, HCT116, HCT116p$^{53-/-}$-DMEM; HRT 18, HRT18SR-RPMI with Geneticin (Gibco) selection.

All treatments were carried out in reduced serum (0.5% FCS) medium for the times and concentrations specified. Aspirin (Sigma) was prepared as previously described[30]. ActinomycinD (Sigma), Cyclohexamide (Sigma), TNF (R&D Systems), ceramide C2/C6 (Sigma), MG132 (Sigma), lactacystin (Calbiochem), quinacrine, Bafilomycin (Sigma) and Calyculin A (Cell Signaling Technology), were all prepared as per manufacturer's instructions. For UV-C treatments, cells were mock treated or exposed to UV-C under the conditions stated. The CDK4 inhibitors 2-bromo-12,13-dihydro-5*H*-indolo[2,3-*a*]pyrrolo[3,4-*c*]carbazole-5,7(6*H*)-dione (CDK4i, Calbiochem) and Palbociclib (PD-0332991, Selleckchem) were solubilised in DMSO as indicated. The rRNA transcription inhibitor BMH-21 (12H-Benzo[g]pyrido[2,1-b]quinazoline-4-carboxamide, N-[2(dimethylamino)ethyl]-12-oxo) was kindly supplied by Prof. Marikki Laiho (Johns Hopkins University School of Medicine, USA) and Nutlin-3 by Prof. Kathryn Ball (University of Edinburgh, Edinburgh Cancer Research Centre, UK).

Immunocytochemistry, image quantification and FUrd assays

Immunocytochemistry was performed as previously described [23]. Primary antibodies were TIF-IA (BioAssayTech), RelA (C-20), Nucelolin (MS-3), RPA194 (all Santa Cruz Biotechnology) and Fibrillarin (Cytoskeleton). Cells were mounted in Vectashield (Vector Laboratories) containing 1ug/ml DAPI. Images were captured using a Coolsnap HQ CCD camera (Photometrics Ltd, Tuscon, AZ, USA) Zeiss Axioplan II fluorescent microscope, 63 × Plan Neofluor objective, a 100□W□Hg source (Carl Zeiss, Welwyn Garden City, UK) and Chroma 83□000 triple band pass filter set (Chroma Technology, Bellows Falls, UT, USA). Image capture was performed using scripts written for IPLab Spectrum 3.6 or iVision 3.6 in

house. For each experiment, a constant exposure time was used. Image quantification was carried out using DAPI as a nuclear marker and fibrillarin as a nucleolar marker along with ScanR (Olympus), IPLab or ImageJ, image analysis software. At least 150 cells from at least 5 random fields of view were quantified for three independent experiments, or as specified in the text.

For fluorouridine (FUrd) run on assays, cells were treated with 2mM FUrd 15min before harvest. Immunocytochemistry was then performed with an anti-BrdU antibody (Sigma). Images were captured using a ScanR high-content imager (Olympus) with a LUCPLFLN 40X objective (Olympus) and ScanR Acquisition software (Olympus). FUrd incorporation was quantified for at least 1000 cells per slide using ScanR analysis software with particle recognition algorithms.

Plasmids, siRNA and transfections

Flag-UBF wild type, S388G and S484A mutants were kindly provided by R. Voit (German Cancer Research Centre, Heilderberg, Germany)[25]. NF-κB reporter constructs (3 x enhancer κB ConA (3x κB ConA-Luc), IκBα luciferase (IκBα-Luc)) and ΔB-deleted derivatives (ΔκB ConA-Luc, ΔIκBα-Luc) were provided by RT Hay (University of Dundee, Dundee, UK) and have been described elsewhere. pCMV-β is commercially available (Promega). pEGFP-C1-hTIF-IA was kindly gifted by I Grummt (German Cancer Research Centre, Heilderberg, Germany). TIF-IA deletion mutants were generated by PCR subcloning TIF-IA fragments corresponding to amino acids 94-204, 94-302, 94-403 and 94-651 in fusion with GFP in the pEGFP-C1 (Clonetech) vector. TIF-IA site mutants were generated using pEGFP-C1-hTIF-IA as a template and QuikChange site directed mutagenesis (Agilent Technologies). The sequence of all constructs was confirmed. Flag-P14ARF was gifted by A Lamond (University of Dundee, Dundee, UK).

siRNA duplex oligonucleotides were synthesized by MWG and transfected into cells using lipofectamine 2000 following the manufacturer's instructions. Cells were transfected on two consecutive days then left to recover for 24-48h prior to treatment or harvest. siRNA sequences are given in full in supplemental data.

Quantitative PCR

RNA was extracted from cells using RNeasy mini kit (Qiagen) following the manufacturer's instructions. Extracted RNA was purified using RQ1 RNase-free DNase (Promega) then cDNA generated using 1st Strand cDNA synthesis kit (Roche). Taqman assays (Thermo Fisher Scientific) and a LightCycler 480 system were used to quantify transcript levels. Primers and probes used in taqman gene expression assay are given in full in additional information. The Comparative C_T Method (or $\Delta\Delta C_T$ Method) was used for calculation of relative gene expression.

Immunoblotting, luciferase reporter and apoptosis assays

Immunoblotting, luciferase reporter and AnnexinV apoptosis assays were carried out as described previously[23, 30]. Primary antibodies used for immunoblots are described in full in supplemental data.

Immunoprecipitation

Immunoprecipitation assays were performed using 1mg whole cell lysate, prepared in NP40 lysis buffer. Mouse TIF-IA antibody (Santa Cruz Biotechnology) was used to immunoprecipitate the appropriate protein. Mouse IgG (pre-immune serum) was used as a control. Complexes were resolved by SDS polyacrylamide gel electrophoresis then analysed by western blot analysis.

Ex vivo treatment of tumour biopsies and immunohistochemistry

Biopsies of colorectal tumours were provided by a pathologist at the time of resection. All patients were consented and full ethical approval was in place (Scottish Colorectal Cancer

Genetic Susceptibility Study 3; Reference: 11/SS/0109). Biopsies were immediately transferred to the lab immersed in culturing media (MEM supplemented with glutamine, penicillin/streptomycin and anti-mycotic/antibiotic mix (1:100, Sigma). Tumours were washed, dissected into 1-2mM fragments then plated. Treatment (0-100μM aspirin, 1h, 37^{o}C) of tumour explants was performed in 96-well plates in duplicate in the presence of 10% foetal calf serum. Following treatment, tumours were either frozen for protein analysis (set 1) or formalin fixed for immunohistochemistry (set 2) . Whole cell extracts were prepared using a TissueLyser(Qiagen) and standard whole cell lysis buffer.

Anti-^{p536}RelA immunohistochemistry was carried out using a DAB protocol on formalin fixed sections, as previously described [59]. A Leica scanner digitised images then Leica QWin plus image analysis software (Leica Microsystems Inc., Buffalo, IL) used to analyse cells for nuclear RelA^{p536} staining. Three distinct areas of tissue and at least 1500 cells were analysed per section (average 4650). The quantification software determined the percentage of cells showing negative, weak, moderate and strong RelA^{p536} staining.

Acknowledgements

The work was supported by grants from the WWCR (formally AICR 10-0158 to LS), Rosetrees trust (A631 and JS16/M225 to LS), BBSRC (case studentship to LS for SN) and MRC (MR/J001481/1). JC and IL were supported by University of Edinburgh scholarships. We would like to thank RT. Hay (University of Dundee), A Lamond (University of Dundee), I Grummt (German Cancer Centre), H Bierhoff (German Cancer Centre), M Laiho (Johns Hopkins University School of Medicine) and B McStay (NUI Galway) for providing tools and reagents. We would also like to thank Nick Hastie, Neil Perkins, Arkadiusz Welman and Wendy Bickmore for critically reading the manuscript. C Nicol provided help with figure preparation, ECMC Edinburgh with tissue collection and M. Walker with general laboratory support.

1. Boulon,S., Westman,B.J., Hutten,S., Boisvert,F.M., & Lamond,A.I. The Nucleolus under Stress. *Mol. Cell* **40**, 216-227 (2010).

2. Grummt,I. The nucleolus-guardian of cellular homeostasis and genome integrity. *Chromosoma*(2013).

3. Andersen,J.S. *et al.* Nucleolar proteome dynamics. *Nature* **433**, 77-83 (2005).

4.Boisvert,F.M., van Koningsbruggen,S., Navascues,J., & Lamond,A.I. The multifunctional nucleolus. *Nat. Rev. Mol. Cell Biol.* **8**, 574-585 (2007).

5. Rubbi,C.P. & Milner,J. Disruption of the nucleolus mediates stabilization of p53 in response to DNA damage and other stresses. *EMBO J.* **22**, 6068-6077 (2003).

6. Deisenroth,C. & Zhang,Y. Ribosome biogenesis surveillance: probing the ribosomal protein-Mdm2-p53 pathway. *Oncogene* **29**, 4253-4260 (2010).

7. Woods,S.J., Hannan,K.M., Pearson,R.B., & Hannan,R.D. The nucleolus as a fundamental regulator of the p53 response and a new target for cancer therapy. *Biochim. Biophys. Acta* **1849**, 821-829 (2015).

8. James,A., Wang,Y., Raje,H., Rosby,R., & DiMario,P. Nucleolar stress with and without p53. *Nucleus.* **5**, 402-426 (2014).

9.Moore,H.M. *et al.* Quantitative proteomics and dynamic imaging of the nucleolus reveal distinct responses to UV and ionizing radiation. *Mol. Cell Proteomics.* **10**, M111 (2011).

10. Boisvert,F.M., Lam,Y.W., Lamont,D., & Lamond,A.I. A quantitative proteomics analysis of subcellular proteome localization and changes induced by DNA damage. *Mol. Cell Proteomics*. **9**, 457-470 (2010).

11.Hayden,M.S. & Ghosh,S. NF-kappaB, the first quarter-century: remarkable progress and outstanding questions. *Genes Dev.* **26**, 203-234 (2012).

12. Karin,M. How NF-kappaB is activated: the role of the IkappaB kinase (IKK) complex. *Oncogene* **18**, 6867-6874 (1999).

13. Pahl,H.L. Activators and target genes of Rel/NF-kappaB transcription factors. *Oncogene* **18**, 6853-6866 (1999).

14. Perkins,N.D. The diverse and complex roles of NF-kappaB subunits in cancer. *Nat. Rev. Cancer* **12**, 121-132 (2012).

15. DiDonato,J.A., Mercurio,F., & Karin,M. NF-kappaB and the link between inflammation and cancer. *Immunol. Rev.* **246**, 379-400 (2012).

16. Nguyen le,X.T. & Mitchell,B.S. Akt activation enhances ribosomal RNA synthesis through casein kinase II and TIF-IA. *Proc. Natl. Acad. Sci. U. S. A* **110**, 20681-20686 (2013).

17. Wu,S. & Tong,L. Differential signaling circuits in regulation of ultraviolet C light-induced early- and late-phase activation of NF-kappaB. *Photochem. Photobiol.* **86**, 995-999 (2010).

18. Li,N. & Karin,M. Ionizing radiation and short wavelength UV activate NF-kappaB through two distinct mechanisms. *Proc. Natl. Acad. Sci. U. S. A* **95**, 13012-13017 (1998).

19. Bierhoff,H., Dundr,M., Michels,A.A., & Grummt,I. Phosphorylation by casein kinase 2 facilitates rRNA gene transcription by promoting dissociation of TIF-IA from elongating RNA polymerase I. *Mol. Cell Biol.* **28**, 4988-4998 (2008).

20. Kato,T., Jr., Delhase,M., Hoffmann,A., & Karin,M. CK2 Is a C-Terminal IkappaB Kinase Responsible for NF-kappaB Activation during the UV Response. *Mol. Cell* **12**, 829-839 (2003).

21. Jiang,H.Y. *et al.* Phosphorylation of the alpha subunit of eukaryotic initiation factor 2 is required for activation of NF-kappaB in response to diverse cellular stresses. *Mol. Cell Biol.* **23**, 5651-5663 (2003).

22. Goldstein,E.N., Owen,C.R., White,B.C., & Rafols,J.A. Ultrastructural localization of phosphorylated eIF2alpha [eIF2alpha(P)] in rat dorsal hippocampus during reperfusion. *Acta Neuropathol.* **98**, 493-505 (1999).

23. Stark,L.A. & Dunlop,M.G. Nucleolar sequestration of RelA (p65) regulates NF-kappaB-driven transcription and apoptosis. *Mol. Cell Biol.* **25**, 5985-6004 (2005).

24. Khandelwal,N. *et al.* Nucleolar NF-kappaB/RelA mediates apoptosis by causing cytoplasmic relocalization of nucleophosmin. *Cell Death. Differ.* **18**, 1889-1903 (2011).

25. Voit,R. & Grummt,I. Phosphorylation of UBF at serine 388 is required for interaction with RNA polymerase I and activation of rDNA transcription. *Proc. Natl. Acad. Sci. U. S. A* **98**, 13631-13636 (2001).

26. Drygin,D. *et al.* Targeting RNA polymerase I with an oral small molecule CX-5461 inhibits ribosomal RNA synthesis and solid tumor growth. *Cancer Res.* **71**, 1418-1430 (2011).

27. Peltonen,K. *et al.* A targeting modality for destruction of RNA polymerase I that possesses anticancer activity. *Cancer Cell* **25**, 77-90 (2014).

28. Mayer,C., Bierhoff,H., & Grummt,I. The nucleolus as a stress sensor: JNK2 inactivates the transcription factor TIF-IA and down-regulates rRNA synthesis. *Genes Dev.* **19**, 933-941 (2005).

29. Mayer,C., Zhao,J., Yuan,X., & Grummt,I. mTOR-dependent activation of the transcription factor TIF-IA links rRNA synthesis to nutrient availability. *Genes Dev.* **18**, 423-434 (2004).

30. Stark,L.A., Din,F.V.N., Zwacka,R.M., & Dunlop,M.G. Aspirin-induced activation of the NF-kB signalling pathway: A novel mechanism for aspirin-mediated apoptosis in colon cancer cells. FASEB J . http://www.fasebj.org/content/early/2001/05/02/fj.00-0529fje.long (2001)

31. Charruyer,A. *et al.* UV-C light induces raft-associated acid sphingomyelinase and JNK activation and translocation independently on a nuclear signal. *J. Biol. Chem.* **280**, 19196-19204 (2005).

32. Verheij,M. *et al.* Requirement for ceramide-initiated SAPK/JNK signalling in stress-induced apoptosis. *Nature* **380**, 75-79 (1996).

33. Chan,T.A., Morin,P.J., Vogelstein,B., & Kinzler,K.W. Mechanisms underlying nonsteroidal antiinflammatory drug-mediated apoptosis. *Proc. Natl. Acad. Sci. U. S. A.* **95**, 681-686 (1998).

34. Fillet,M. *et al.* Mechanisms involved in exogenous C2- and C6-ceramide-induced cancer cell toxicity. *Biochem. Pharmacol.* **65**, 1633-1642 (2003).

35. Fatyol,K. & Grummt,I. Proteasomal ATPases are associated with rDNA: the ubiquitin proteasome system plays a direct role in RNA polymerase I transcription. *Biochim. Biophys. Acta* **1779**, 850-859 (2008).

36. Yuan,X., Zhao,J., Zentgraf,H., Hoffmann-Rohrer,U., & Grummt,I. Multiple interactions between RNA polymerase I, TIF-IA and TAF(I) subunits regulate preinitiation complex assembly at the ribosomal gene promoter. *EMBO Rep.* **3**, 1082-1087 (2002).

37. Ayrault,O. *et al.* Human tumor suppressor p14ARF negatively regulates rRNA transcription and inhibits UBF1 transcription factor phosphorylation. *Oncogene* **25**, 7577-7586 (2006).

38. Rocha,S., Campbell,K.J., & Perkins,N.D. p53- and Mdm2-independent repression of NF-kappa B transactivation by the ARF tumor suppressor. *Mol. Cell* **12**, 15-25 (2003).

39. Thoms,H.C., Dunlop,M.G., & Stark,L.A. p38-mediated inactivation of cyclin D1/cyclin-dependent kinase 4 stimulates nucleolar translocation of RelA and apoptosis in colorectal cancer cells. *Cancer Res.* **67**, 1660-1669 (2007).

40. Voit,R., Hoffmann,M., & Grummt,I. Phosphorylation by G1-specific cdk-cyclin complexes activates the nucleolar transcription factor UBF. *EMBO J.* **18**, 1891-1899 (1999).

41. Cavanaugh,A.H. *et al.* Activity of RNA polymerase I transcription factor UBF blocked by Rb gene product. *Nature* **374**, 177-180 (1995).

42. Din,F.V., Stark,L.A., & Dunlop,M.G. Aspirin-induced nuclear translocation of NFkappaB and apoptosis in colorectal cancer is independent of p53 status and DNA mismatch repair proficiency. *Br. J. Cancer* **92**, 1137-1143 (2005).

43. Rothwell,P.M. *et al.* Long-term effect of aspirin on colorectal cancer incidence and mortality: 20-year follow-up of five randomised trials. *Lancet* **376**, 1741-1750 (2010).

44. Din,F.V. *et al.* Effect of aspirin and NSAIDs on risk and survival from colorectal cancer. *Gut* **59**, 1670-1679 (2010).

45. Cao,Y. *et al.* Population-wide Impact of Long-term Use of Aspirin and the Risk for Cancer. *JAMA Oncol.*(2016).

46. Tsai,R.Y. & Pederson,T. Connecting the nucleolus to the cell cycle and human disease. *FASEB J.* **28**, 3290-3296 (2014).

47. Thoms,H.C., Dunlop,M.G., & Stark,L.A. p38-mediated inactivation of cyclin D1/cyclin-dependent kinase 4 stimulates nucleolar translocation of RelA and apoptosis in colorectal cancer cells. *Cancer Res.* **67**, 1660-1669 (2007).

48. Negi,S.S. & Brown,P. Transient rRNA synthesis inhibition with CX-5461 is sufficient to elicit growth arrest and cell death in acute lymphoblastic leukemia cells. *Oncotarget.* **6**, 34846-34858 (2015).

49. Thoms,H.C., Dunlop,M.G., & Stark,L.A. CDK4 inhibitors and apoptosis: a novel mechanism requiring nucleolar targeting of RelA. *Cell Cycle* **6**, 1293-1297 (2007).

50. Bywater,M.J. *et al.* Inhibition of RNA polymerase I as a therapeutic strategy to promote cancer-specific activation of p53. *Cancer Cell* **22**, 51-65 (2012).

51. Birbach,A., Bailey,S.T., Ghosh,S., & Schmid,J.A. Cytosolic, nuclear and nucleolar localization signals determine subcellular distribution and activity of the NF-kappaB inducing kinase NIK. *J. Cell Sci.* **117**, 3615-3624 (2004).

52. Mayer,C. & Grummt,I. Cellular stress and nucleolar function. *Cell Cycle* **4**, 1036-1038

(2005).

53. Bailly,A. *et al.* The NEDD8 inhibitor MLN4924 increases the size of the nucleolus and activates p53 through the ribosomal-Mdm2 pathway. *Oncogene* **35**, 415-426 (2016).

54. Szymanski,J. *et al.* Dynamic subcellular partitioning of the nucleolar transcription factor TIF-IA under ribotoxic stress. *Biochim. Biophys. Acta* **1793**, 1191-1198 (2009).

55. Lessard,F. *et al.* The ARF tumor suppressor controls ribosome biogenesis by regulating the RNA polymerase I transcription factor TTF-I. *Mol. Cell* **38**, 539-550 (2010).

56. Quin,J.E. *et al.* Targeting the nucleolus for cancer intervention. *Biochim. Biophys. Acta* **1842**, 802-816 (2014).

57. Sherr,C.J., Beach,D., & Shapiro,G.I. Targeting CDK4 and CDK6: From Discovery to Therapy. *Cancer Discov.*(2015).

58. Bunz,F. *et al.* Requirement for p53 and p21 to sustain G2 arrest after DNA damage. *Science* **282**, 1497-1501 (1998).

59. Moles,A. *et al.* Inhibition of RelA-Ser536 phosphorylation by a competing peptide reduces mouse liver fibrosis without blocking the innate immune response. *Hepatology* **57**, 817-828 (2013).

Figure 1: Disrupting nucleolar function stimulates the NF-κB pathway

(a) SW480 cells were transfected with Flag tagged wild type (WT) or inactive (S388G) UBF then fixed and immunostained with the indicated antibodies. The nuclear intensity of RelA in Flag positive, and negative cells was quantified using IPlab software and DAPI as a nuclear marker. The mean+/-SEM is shown (N=3). **(b)** Immunoblot analysis was performed on cytoplasmic and nuclear extracts with antibodies to pRelA^{536} and Flag tag respectively. Actin acts as a control. **(c)** Cells transfected as above were co-transfected with an NF-κB reporter (3x κB ConA-luciferase) and control (pCMVβ) plasmid. Graph depicts the relative luciferase activity of UBF-S388G transfected cells compared to those transfected with UBF-WT. Mean of two experiments +/-SEM is shown. **(d)** SW480 cells were transfected with the indicated siRNA species along with pCMVβ and either 3x κB ConA-Luc or the control ConAΔκB-Luc (with κB sites deleted). TNF (10ng/Ml, 4h) acts as a control NF-κB stimulant. Graph depicts % relative luciferase activity compared to cells transfected with control siRNA. The mean of at least three individual repeats (+/-SEM) is shown. Inset: Immunoblot demonstrating levels of pRelA^{536}, nuclear RelA and UBF in whole cell (WCL) and nuclear lysates upon UBF depletion. Actin acts as a control. **(e)** Immunoblot showing cytoplasmic levels of the indicated NF-κB pathway proteins upon siRNA depletion of PolR1A (RPA194) and TIF-IA. Nuclear extracts confirm efficient protein depletion. Tubulin and fibrillarin act as protein loading controls. **(f)** SW480 cells were transfected with the indicated siRNA species along with IκB-luc (luciferase driven by full length IκB promoter) or ΔκB-IκB-luc (equivalent in which NF-κB sites are deleted) and pCMVβ. The percentage relative luciferase activity compared to control siRNA was calculated. Mean+/- SEM is shown (N=3). **(g)** HCT116 cells were transfected with the indicated siRNA species. qRT-PCR with primers for the NF-κB target genes IκB and Bcl-xl, measured gene transcription. GAPDH was used as a normalising gene. Results are presented as the fold induction compared to control siRNA. The mean (+/-

SEM) is shown. N=3. **(h)** SW480 cells were transfected with 3x κB ConA-luc and pCMVβ control. Twentyfour hours later cells were treated with the specified PolI inhibitors CX5461 (500nM), BMH-21 (4uM), ActinomycinD (ActD, 1ug/ml) or the NF-κB stimulant,TNF (10ng/ml), for 5h or as indicated. Relative luciferase activity was assayed as above. Graph depicts the mean of at least three individual repeats +/-SEM. **(i)** Parental HRT18 cells (IκB WT), and cells expressing mutant IκB resistant to stimuli-induced degradation (IκB-SR), were transfected with the indicated siRNA species, pCMVβ and 3x κB ConA-Luc. Relative luciferase activity was determined as in b. Results are presented as percentage of control siRNA. Graph depicts the mean of at least three individual repeats +/-SEM. *P* values throughout are compared to the respective control and were derived using a two tailed students T test. *<0.05, **≤ 0.01, ***≤0.005. Scale bars =10um. See also Supplemental Fig. 1.

Figure 2. Stress-stimuli of the NF-κB pathway induce degradation of TIF-IA and a distinct nucleolar phenotype

(a and b) SW480 cells were treated with aspirin (10mM) for the indicated times **(a)** Top: Immunoblot analysis of p649 phosphorylated and native TIF-IA in WCE. Botom: Immunomicrographs (63X) showing levels and localisation of native TIF-IA. Inset: ImageJ software was used to quantify the percentage of nuclei (as depicted by DAPI stain) with bright puncti of TIF-IA. A minimum of 200 nuclei were analysed per experiment from 10 fields of view. N=3. **(b)** Top: Immunoblot showing cytoplasmic levels of IκBα and control protein (Cu/ZnSOD). Bottom: Immunomicrographs (X63) demonstrating localisation of RelA. Nuclear accumulation can be seen at 2h post treatment. **(c)** SW480 cells were treated with cyclohexamide (10uM) alone or with aspirin (10mM) for the times specified. Immunoblot indicates the levels of TIF-IA. See supplemental Fig. 2 for quantification of band intensities. **(d)** SW480 cells were mock or UV-C (40 J/m^2) irradiated. Western blot was

performed on WCE with the indicated antibodies. **(e)** SW480 cells were treated with DMSO (NT), CX5461 (500nM), BMH-21 (4uM), ActinomycinD (ActD, 1ug/ml) or aspirin (10mM) for 4 hours, or TNF (10ng/ml) for 30mins, WCE were examined by western blot using the indicated antibodies. **(f)** qRT-PCR measurement of 47S pre-rRNA transcription in response to aspirin (3mM, 16h) or actinocycinD (50ng/ml, 2h). GAPDH was used as a normalising gene. Results are presented as the percentage of relative 47S transcription compared to non-treated (NT) control. The mean (+/- SEM) is shown. N=4. **(g)** Representative immunomicrographs (x63) showing the cellular localisation of components of the tripartite nucleolar structure in response to aspirin (10mM, 8h) and actinomycinD (50ng/ml). Fibrillarin marks the dense fibrillar component (DFC) and RPA194 the PolI complex in the fibrillar centre. **(h)** DIC immunomicrographs of cells treated as above. Nucleolar area was determined by Image J quantification of fibrillarin staining. Graphs depict the mean (+/- SEM) of at least 250 cells per experiment (N=3). **(i)** Changes in rRNA transcription (compared to time 0) and nucleolar size were monitored over time in SW480 cells using qRTPCR for the 47S transcript (as in f) and ImageJ analysis of area devoid of DAPI staining (as a marker for nucleoli). Graph depicts the mean (+/-SEM). N=3. **(j)** Immunomicrograph (x63) showing the cellular localisation of nucleolin in SW480 cells in response to aspirin (3mM, 16h), UV-C (40j/m^2, 2h) and TNF (10 ng/ml, 1 h). **(k)** SW480 cells were treated with carrier (DMSO), ceramide-2 (C2, 10uM)) or ceramide-6 (C6, 10uM). Top: WCE were analysed by western blot with the indicated antibodies. Bottom: Immunomicrograph (X63) shows the localisation of fibrillarin. Actin was used throughout to control for protein loading and DAPI to identify nuclei. *P* values are compared to the respective control and were derived using a two tailed students T test. ***≤0.005. Scale bars=10uM. See also supplemental Fig 2.

Figure 3: p14ARF facilitates TIF-IA degradation in response to stress

(a) SW480 cells were pre-treated for 2h with DMSO (carrier), MG132 (25uM), Quinacrine (25uM) or MG132 plus quinacrine, then treated with aspirin (10mM, 4h). TIF-IA levels were monitored by Western blot analysis. **(b)** Deletions and specific amino acid mutations were generated in GFP-TIF-IA 1-650 (full length). SW480 cells were transfected with the indicated constructs then treated with aspirin (10mM) for the times specified. Top:Anti-GFP immunoblot was performed on WCE. Bottom: Immunomicrographs (63X) depicting the cellular localisation of GFP-tagged TIF-IA. **(c)** SW480 cells were transfected with pcDNA-3 (control (-)) or pcDNA3-p14ARF (+) then either non-treated or treated with aspirin (3mM 16h). Immmunoblot was performed on WCE with the indicated antibodies. **(d and e)** SW480 cells were transfected with control or p14ARF siRNA then treated with aspirin (0-5mM, 16h). **(d)** Immunoblot analysis was performed on WCE with the indicated antibodies. **(e)** Immunomicrographs (X63) show the levels and localisation of TIF-IA in fixed cells. IPlab software was used to quantify nuclear (as depicted by DAPI staining) intensity of TIF-IA. Data are the mean (+/-SEM) of >150 nuclei. N=3. Inset shows nucleolar (outlined) accumulation of TIF-A in p14ARF transfected cells treated with aspirin. **(f)** SW480 cells were treated with 0-5mM aspirin for 16h. Immunoprecipitation was carried out on WCE using antibodies to TIF-IA and IgG control. Precipitated proteins were subjected to western blot analysis with the indicated antibodies. Input levels are shown. Actin was used throughout to control for protein loading and DAPI to identify nuclei. *P* values are compared to the respective control and were derived using a two tailed students T test. ***≤0.005. Scale bars=10uM. See also supplemental Fig 3.

Figure 4. CDK4 inhibition-UBF lie upstream of stress-mediated TIF-IA degradation

(**a to g**) SW480 (or Hela (**b**)) cells were treated with carrier (DMSO), aspirin (3mM, 16h) or the small molecule CDK4 inhibitor, 2-bromo-12,13-dihy-dro-indolo[2,3-a]pyrrolo[3,4-c]

carbazole-5,7(6H)-dione (CDK4i, 2uM or as indicated). **(a and b)** Anti-TIF-IA immunoblot performed on WCE from (**a**) SW480 or (**b**) Hela cells. **(c)** Immunomicrographs (63X) demonstrating the levels and localisation of TIF-IA. Arrows indicate cytoplasmic localisation at lower dose. (d) Immunomicrograph (63X) depicting the localisation of fibrillarin. **(e and f)** SW480 cells were transfected with control or p14ARF siRNA 72hs prior to treatment. **(e)** Western blot was performed with the indicated antibodies. **(f)** Immunomicrographs (X63) showing the levels/localisation of TIF-IA. **(g)** Immunoblot demonstrating levels of S484 phosphorylated and native UBF, in relation to TIF-IA, in response to treatment. **(h)** SW480 cells were transfected with control, UBF or PolIRIA siRNA then treated with aspirin or CDK4i as in **a**. Western blot analysis was performed with the indicated antibodies. **(i)** SW480 cells were transfected with control or UBF siRNA then either mock transfected or transfected with Flag-UBF-wild type (WT) or the S484A phospho-mutant. 8hs later, transfected cells were treated with CDK4i (2uM, 16h). Immunoblot was performed with the indicated antibodies.

Figure 5. TIF-IA degradation is causally linked to increased nucleolar area and stimulation of the NF-κB pathway

(a to e) SW480 cells were transfected with control or p14ARF siRNA as in Figure 4 then treated with aspirin or CDK4i (16h) at the concentrations specified. **(a)** Immunocytochemistry was performed on fixed cells with the indicated antibodies. Below: The percentage of cells in the population showing nucleolar RelA (p65) was quantified for at least 6 fields of view (>100 cells)/experiment. Nucleolar area was quantified using IPlab software with fibrillarin as a nucleolar marker. Mean (+/- SEM) of three individual experiments is shown. **(b)** Immunoblot demonstrating cytoplasmic levels of IκBα. **(c)** Immunocytochemistry was performed as in (a). Arrow indicates nuclear RelA. **(d)** Immunoblot was performed with indicated antibodies. **(e)** Annexin V-FITC apoptosis assays

were used to identify apoptotic cells. Microscopy was used to determine the number of cells (identified by DAPI counterstain) undergoing apoptosis. At least 200 cells from a minimum of 10 independent fields of view were analysed. Graph shows mean of 3 experiments (+/- SEM). **(f)** SW480 cells were transfected with the specified siRNA species then co-transfected with Flag-UBF WT or Flag UBF^{S484A} expression vectors. Immunomicrograph demonstrates the localisation of RelA after CDK4i (2uM, 16h) treatment. Below: ImageJ was used to quantify the nuclear (as depicted by DAPI staining) intensity of RelA. Graph depicts the mean of at least 200 cells/experiment (+/- SEM). See also supplemental Fig. 4. **(g)** Based on our data we propose the outlined model. See text for details. Scale bars=10um. Actin was used as a loading control. P values were derived using a two tailed students Ttest. *<0.05, **<0.01, ***<0.005. NS-non significant. See also supplemental figure 5.

Figure 6 TIF-IA degradation correlates with NF-κB pathway activation in human clinical samples

(a) Diagram depicting workflow of *ex vivo* culture. Taken from (O' Hara et al, 2014). Resected colorectal tumour biopsies were immediately transferred to the lab, washed, immersed in culturing media in 96 well plates then exposed to 0-100uM aspirin for 1h. One piece of tissue was fixed for immunohistochemistry, while another was frozen for protein analysis. This was carried out for 7 patients. **(b)** Immunoblot analysis was performed on whole cell lysates with the indicated antibodies. Image J was used to quantify the intensity of TIF-IA relative to actin. *= Tumours showing a greater than 2 fold decrease in relative levels of TIF-IA. **(c)** Immunohistochemistry was performed on sections from paraffin embedded tissue with antibodies to RelA^{p536}. Images were digitised then Leica QWin plus image analysis software used to quantify the nuclear RelA^{p536} intensity. Three distinct areas of tissue and at least 1500 cells were analysed per section. Data presented are the % cells showing moderate+strong RelA ^{p536} staining, as indicated by image analysis software. Top: an example

immunomicrograph. Arrows indicates epithelial cells. Bottom: Quantification data. * Significant ($P<0.05$) difference between the % stained cells in treated and non-treated sections. **(d)** Graph showing the relationship between aspirin-induced changes in TIF-IA and $RelA^{p536}$ staining for 6 individual tumours.

Figure 1

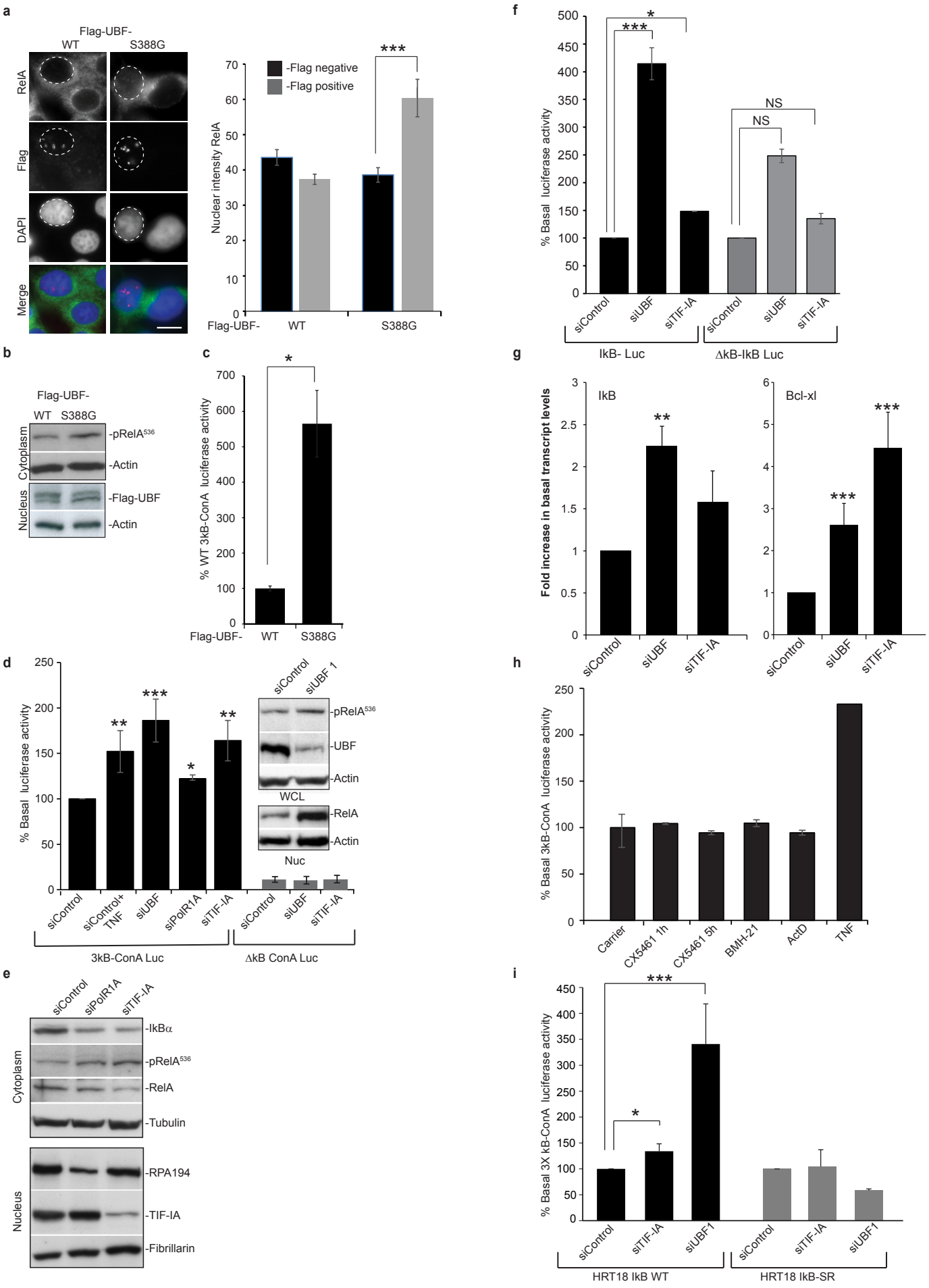

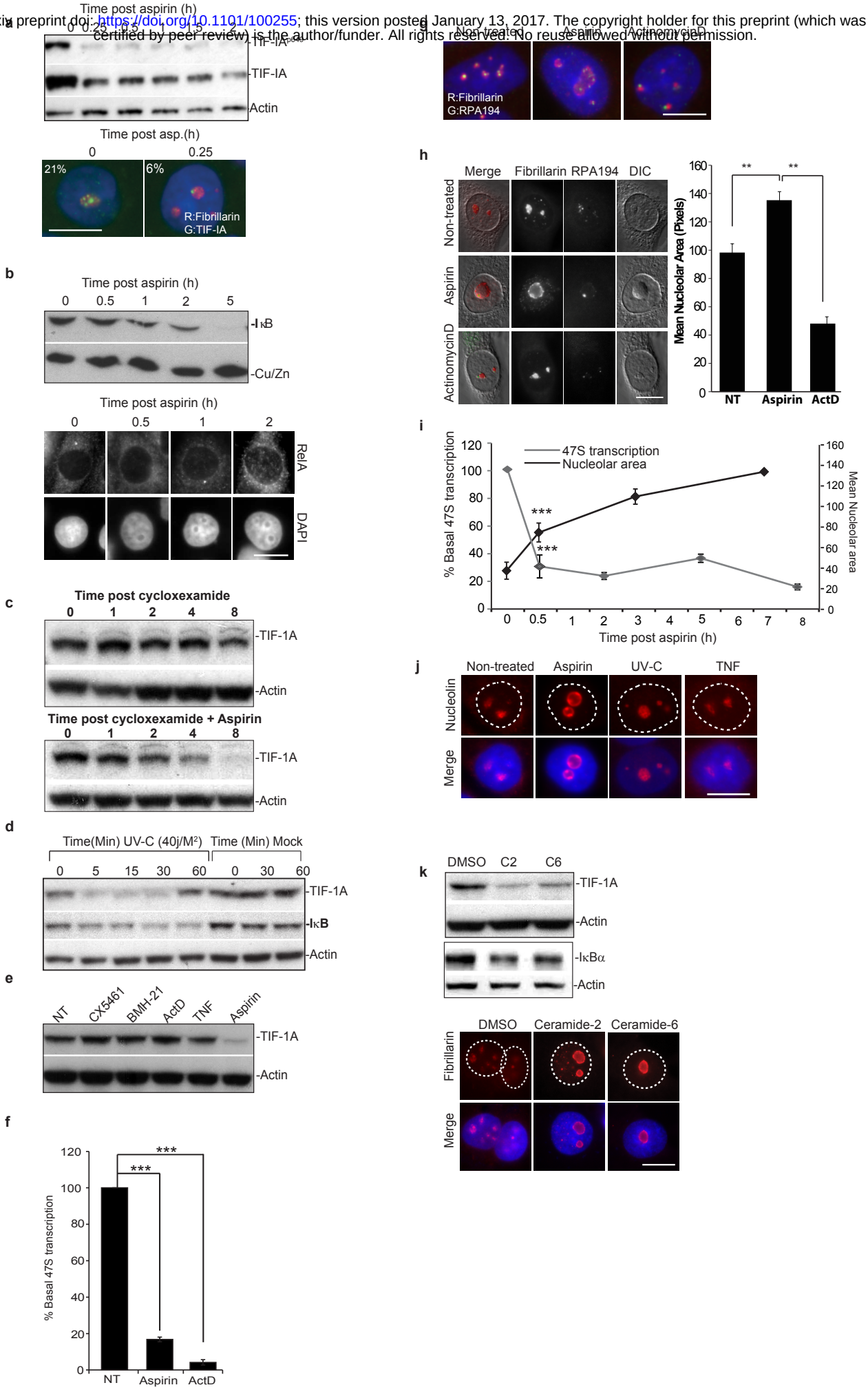

Figure 3

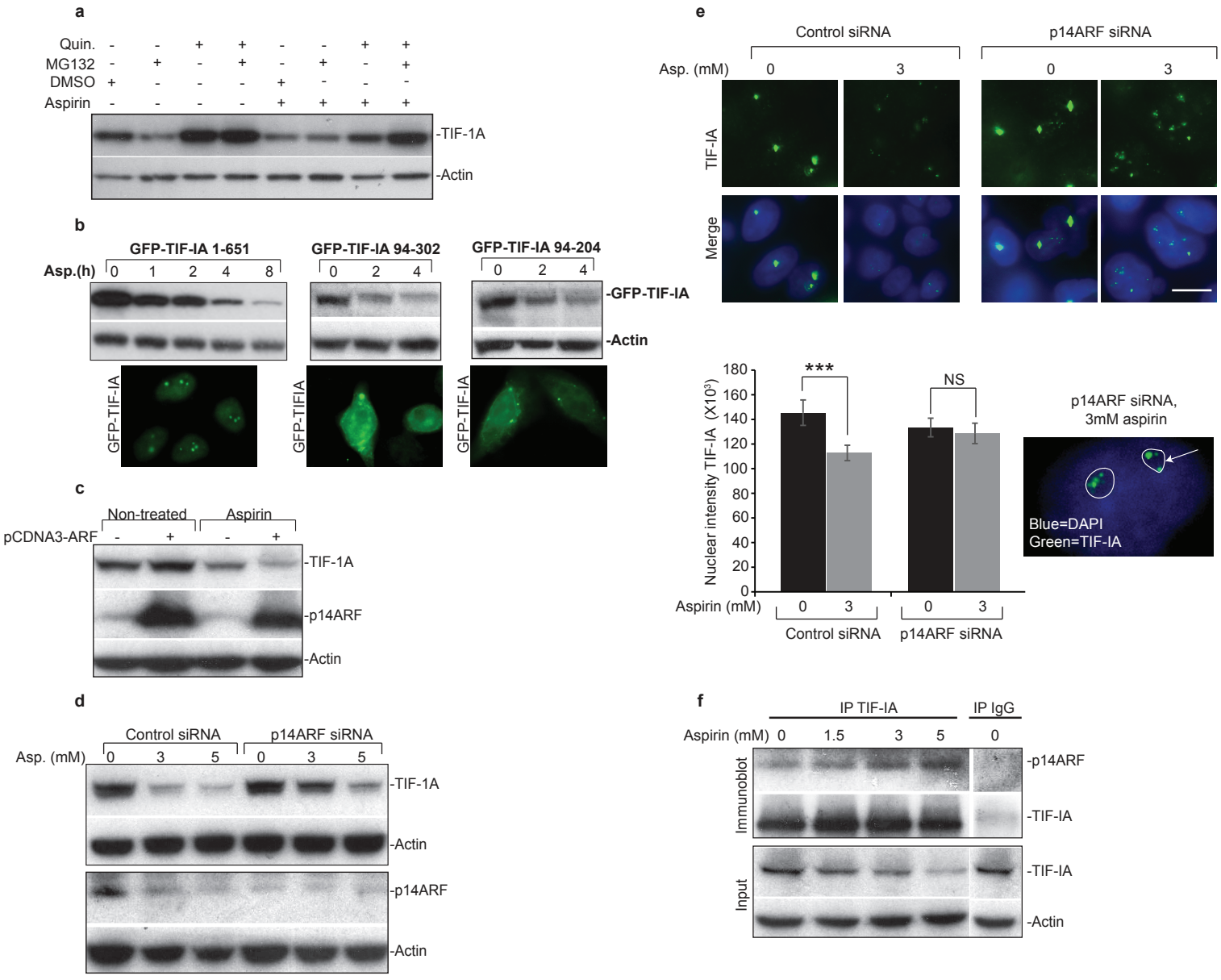

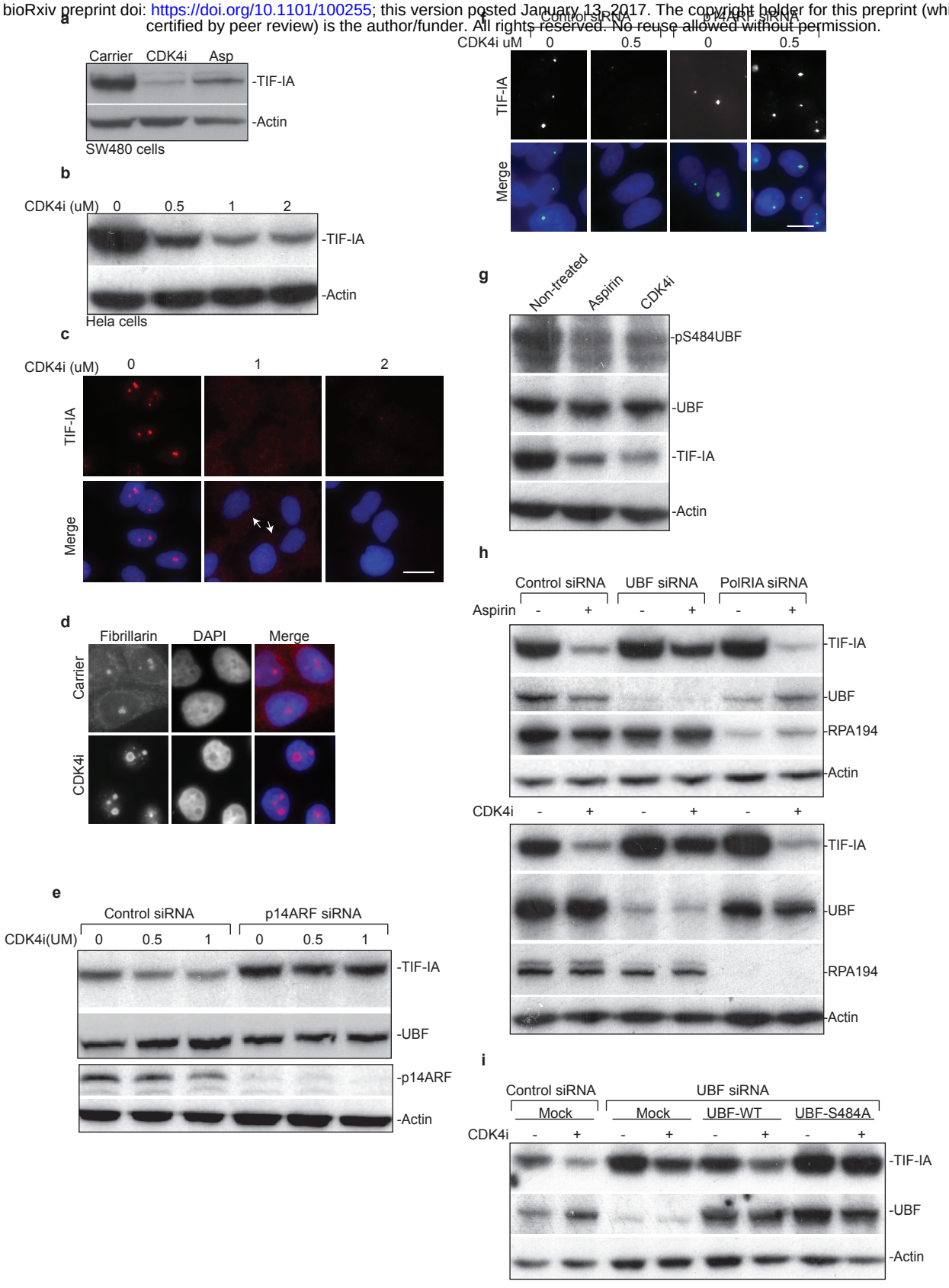

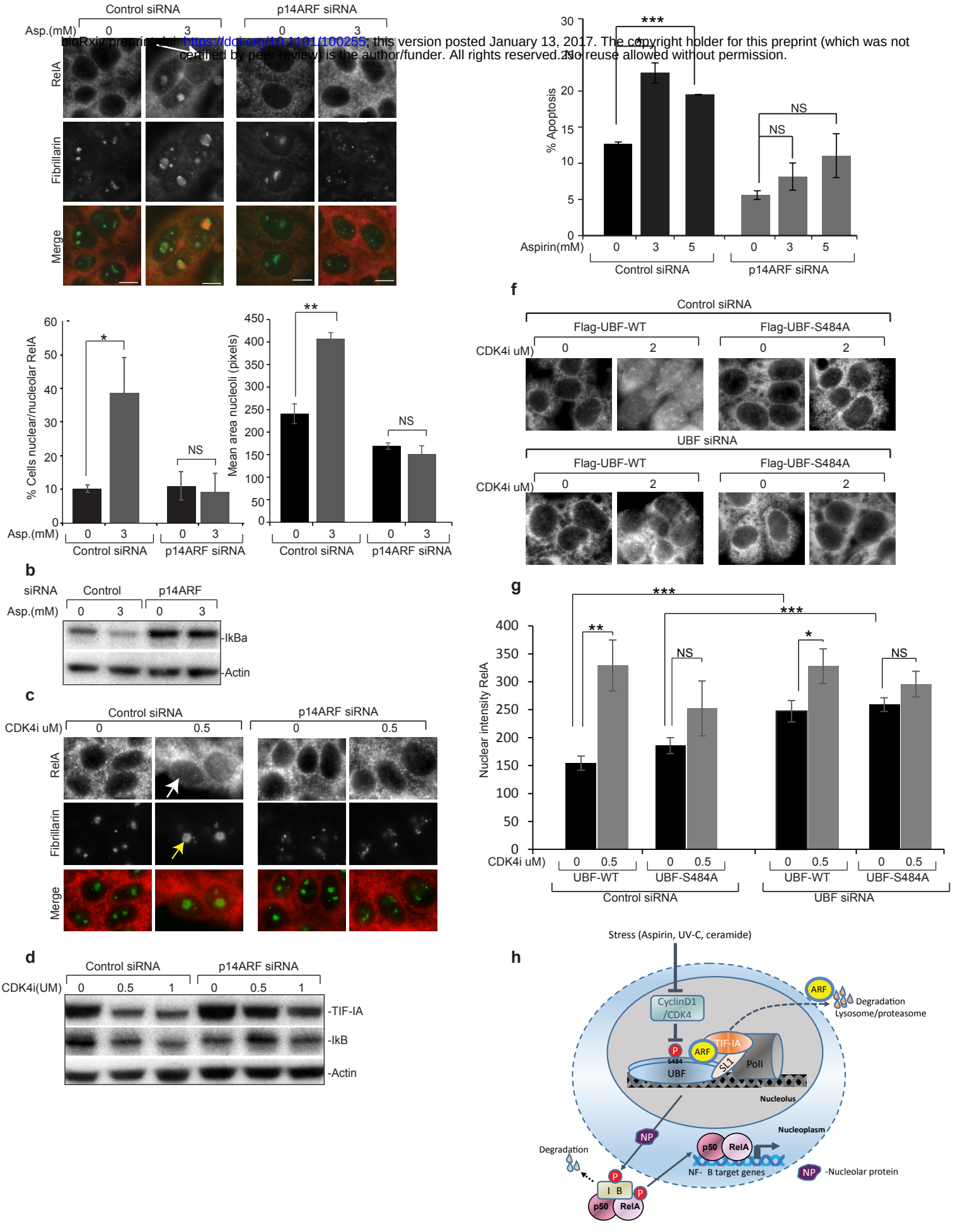

Figure 6